

# Comparative study of excitonic structures and luminescence properties of $\text{Bi}_4\text{Ge}_3\text{O}_{12}$ and $\text{Bi}_{12}\text{GeO}_{20}$

Minoru Itoh<sup>\*1</sup>, Tsuyoshi Katagiri<sup>1</sup>, Hiroyuki Mitani<sup>1</sup>, Masami Fujita<sup>2</sup>, and Yoshiyuki Usuki<sup>3</sup>

<sup>1</sup> Department of Electrical and Electronic Engineering, Shinshu University, Nagano 380-8553, Japan

<sup>2</sup> Japan Coast Guard Academy, Wakaba, Kure 737-8512, Japan

<sup>3</sup> Furukawa Co., Kannondai, Tsukuba 305-0856, Japan

Received 11 June 2008, revised 22 July 2008, accepted 23 July 2008

Published online 15 October 2008

PACS 71.20.Ps, 71.35.Cc, 78.40.Ha, 78.55.Hx

\* Corresponding author: e-mail: itohlab@shinshu-u.ac.jp, Phone: +81 26 269 5261, Fax: +81 26 269 5220

The measurements of reflection, emission-excitation, luminescence decay kinetics, and x-ray photoelectron of  $\text{Bi}_4\text{Ge}_3\text{O}_{12}$  and  $\text{Bi}_{12}\text{GeO}_{20}$  crystals have been performed, in addition to relativistic molecular orbital calculations. Both materials consist of the same elements but form different crystal structure. Based on the obtained results, the excitonic reflection structures and luminescence properties of  $\text{Bi}_4\text{Ge}_3\text{O}_{12}$  and  $\text{Bi}_{12}\text{GeO}_{20}$  are discussed in comparison with each other.

Copyright line will be provided by the publisher

**1 Introduction** Bismuth germanate  $\text{Bi}_4\text{Ge}_3\text{O}_{12}$  and bismuth germanium oxide  $\text{Bi}_{12}\text{GeO}_{20}$  are usually abbreviated as BGO in common. The former is a cubic crystal (space group  $I\bar{4}3d$ ) of the eulytine-type structure with the  $\text{Bi}^{3+}$  site coordinated by a distorted octahedron of six oxygen atoms, and is widely used as a scintillation material.[1] The latter is also cubic (space group  $I23$ ) with the sillenite-type structure consisting of the  $\text{Bi}^{3+}$  ions coordinated heptahedrally by oxygen, and has high potential for applications in electro-optic devices.[2] Although the optical properties of  $\text{Bi}_4\text{Ge}_3\text{O}_{12}$  have attracted a great deal of attention,[3-6] interpretation of the reflection and luminescence spectra is still rather controversial, due to the lack of an adequate model for the electronic structure.[7,8] On the other hand, there are only a few papers on the optical properties of  $\text{Bi}_{12}\text{GeO}_{20}$ . [9,10]

In the present work, we have performed the measurements of reflection, emission-excitation, luminescence decay kinetics, and x-ray photoelectron of  $\text{Bi}_4\text{Ge}_3\text{O}_{12}$  (e-BGO) and  $\text{Bi}_{12}\text{GeO}_{20}$  (s-BGO) crystals. The electronic structures of both materials are also studied by a relativistic molecular orbital calculation. A comparison of the results obtained for e-BGO and s-BGO provides useful information on their optical properties.

**2 Experiment** The samples used in the present experiment were freshly cleaved from single-crystalline ingots of e-BGO and s-BGO grown by the Czochralski technique. They were mounted on the sample holder in a closed-cycle He optical cryostat working in the temperature range  $T = 5\text{--}300$  K.

Reflection and emission spectra were examined by using synchrotron radiation from the UVSOR storage ring in Okazaki as a light source. The incident light was monochromatized with a 1-m VUV monochromator of Seya-Namioka type. The reflected light was measured under near-normal incidence. Three dimensional (3D) emission-excitation spectra were obtained using an Acton SpectraPro-300i monochromator equipped with a liquid-nitrogen cooled charge-coupled device camera. The emission spectra were not corrected for the spectral response of the detection system, while the excitation spectra were corrected for the intensity distribution of the incident light.

Luminescence decay kinetics was detected by a photomultiplier and displayed on a digital storage oscilloscope under the excitation with the fourth harmonics (4.66 eV) of a Q-switched Nd:YAG laser. X-ray photoelectron spectroscopy (XPS) was carried out by an ESCA spectrometer, with an excitation source of Al anode ( $K\alpha$ : 1486.6 eV). An electron flood gun was employed to compensate for the sample charging under x-ray irradiation.

**3 Experimental results** Figures 1(a) and 1(b) show the reflection spectra of e-BGO and s-BGO at  $T = 5$  K, respectively. The e-BGO exhibits a sharp lowest-energy peak at 4.81 eV. A weak peak is clearly observable at 5.15 eV in the low-energy region of a strong band at around 6.25 eV. A broad band appears in the region between 12 and 23 eV. In the high-energy region, three distinct peaks are observed at 26.4, 27.8, and 29.7 eV. The s-BGO exhibits a clear peak at 3.65 eV. A strong band consisting of some structures is seen at around 5.0 eV. A broad band with a sharp peak at 14.6 eV appears in the 11–23 eV region. Three distinct peaks are also observed at 26.1, 27.0, and 29.3 eV. The overall structures in Figs. 1(a) and 1(b) are in general agreement with the earlier results for e-BGO [3] and s-BGO [10], respectively.

Figures 2(a) and 2(b) show the contour plots of the 3D emission-excitation spectra of e-BGO and s-BGO at 5 K, respectively. In e-BGO, an intense emission band appears at around 510 nm (2.43 eV). The excitation threshold of the 510 nm band locates at 285 nm (4.35 eV). When  $T$  goes from 5 to 300 K, the peak position blue-shifts toward 490 nm, and the emission intensity decreases to 1/5, in good agreement with the result by Weber and Monchamp [4]. In s-BGO, a broad emission band is observed at 450 nm (2.75 eV), with the excitation threshold at 360 nm (3.44 eV). The 450 nm band disappears at  $T > 50$  K.

The luminescence yield of the 450 nm band in s-BGO at low temperatures is more than one order of magnitude

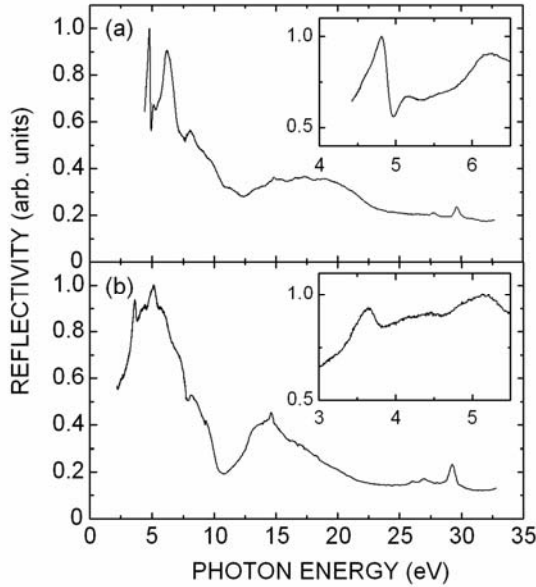


**Figure 1** Reflection spectra of (a) e-BGO and (b) s-BGO at  $T = 5$  K. The insets show the low-energy part in an expanded scale.

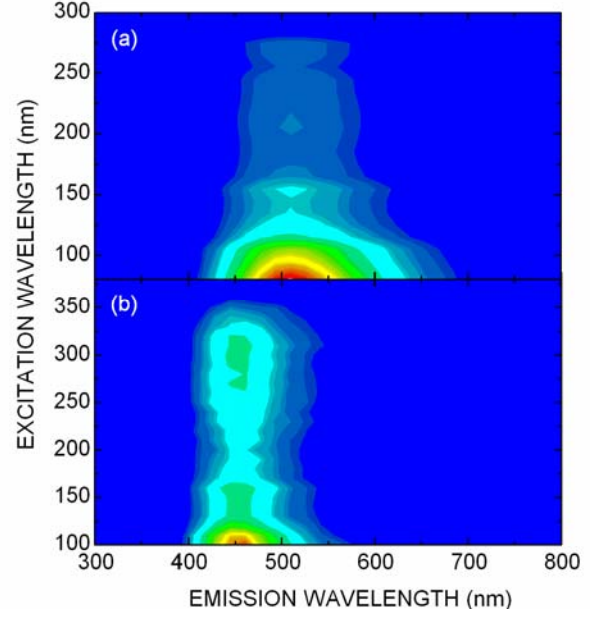


**Figure 2** Contour plot of the 3D emission-excitation spectra of (a) e-BGO and (b) s-BGO at  $T = 5$  K.

weaker than that of the 510 nm band in e-BGO. Furthermore, it is worth noticing that the Stokes shift in s-BGO is considerably smaller than that in e-BGO.

The decay time of the 510 nm luminescence in e-BGO is reported to be 138  $\mu$ s at  $T = 6$  K.[11] Decay kinetics measurements have not been made for the 450 nm luminescence in s-BGO. The result obtained at 8 K is shown in Fig. 3. The decay curve is non-exponential, and is fitted by a sum of three components;  $I(t) = I_f(0)\exp(-t/\tau_f) + I_m(0)\exp(-t/\tau_m) + I_s(0)\exp(-t/\tau_s)$ , with a fast component  $\tau_f \approx 10$  ns, a middle component  $\tau_m \approx 12$   $\mu$ s, and a slow component  $\tau_s \approx 130$   $\mu$ s, as indicated by the red line.

The XPS spectra of e-BGO and s-BGO are presented in Figs. 4(a) and 4(b), respectively. The binding energy is given relative to the top of the valence band. Both spectra exhibit similar structures because of the same constituent atoms. However, there are some differences between Figs. 4(a) and 4(b). An isolated band is seen at around 10 eV in Fig. 4(b). This band is assigned to the Bi 6s state from the theoretical calculation described below. In Fig. 4(a), a similar band is observed at 11.5 eV, but it overlaps with the bottom region of the valence band. The O 2s band appears at 21 eV in Fig. 4(a) and at 20 eV in Fig. 4(b). Two intense peaks due to the Bi 5d state are observed at 25.1 and 28.2 eV in Fig. 4(a) and at 24.3 and 27.4 eV in Fig. 4(b). A band at 30.5 eV is ascribed to the Ge 3d state. This band is strong in Fig. 4(a), while it is weak in Fig. 4(b) because the amount of Ge atoms is relatively small in s-BGO.

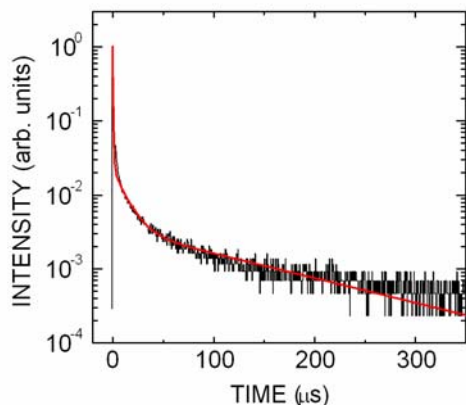


**Figure 3** Decay kinetics of the 450 nm luminescence in s-BGO at  $T = 8$  K. Red line is the best fit of the decay curve consisting of three components to the experimental data.

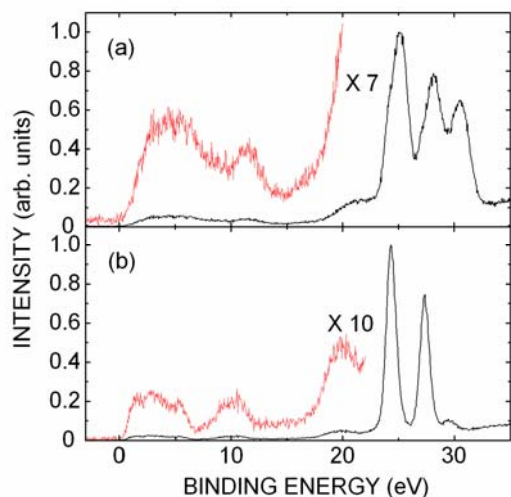


**Figure 4** XPS spectra of (a) e-BGO and (b) s-BGO.

#### 4 Electronic structures calculated by DV- $X\alpha$ method

The electronic structure of e-BGO has been proposed by Moncorge et al.[7] and Lalic et al.[8] There is a significant difference between these two results. The top of the valence band is made of the Bi 6s state in Ref. [7], but is formed by the O 2p state without any contribution from the Bi 6s state in Ref. [8]. The electronic band structure of s-BGO has been calculated by using the local pseudo-potential method. [12]

In our study, the electronic structures of e-BGO and s-BGO were investigated by relativistic molecular orbital calculations using the DV- $X\alpha$  method, the details of which are described in Ref. [13]. Large  $[\text{Bi}_{12}\text{Ge}_9\text{O}_{52}]^{32-}$  and  $[\text{Bi}_{12}\text{GeO}_{28}]^{16-}$  clusters centered at  $[\text{GeO}_4]^{4-}$  were chosen for e-BGO and s-BGO, respectively, by taking the Madelung potentials around the clusters into account.

Figure 5 shows the energy-level diagrams and the partial density of states (PDOS) per molecule for (a) e-BGO and (b) s-BGO. The band-gap energy  $E_g$  is calculated to be 4.79 eV for e-BGO and 3.85 eV for s-BGO. The partial contributions of the electronic states of Bi, Ge, and O atoms to the bottom of the conduction band are 83.0%, 5.0%, and 12.0% in e-BGO and 82.6%, 1.1%, and 16.3% in s-BGO, respectively. The partial contributions of these electronic states to the top of the valence band are 22.6%, 0.5%, and 76.9% in e-BGO and 2.1%, 0.1%, and 97.8% in s-BGO.

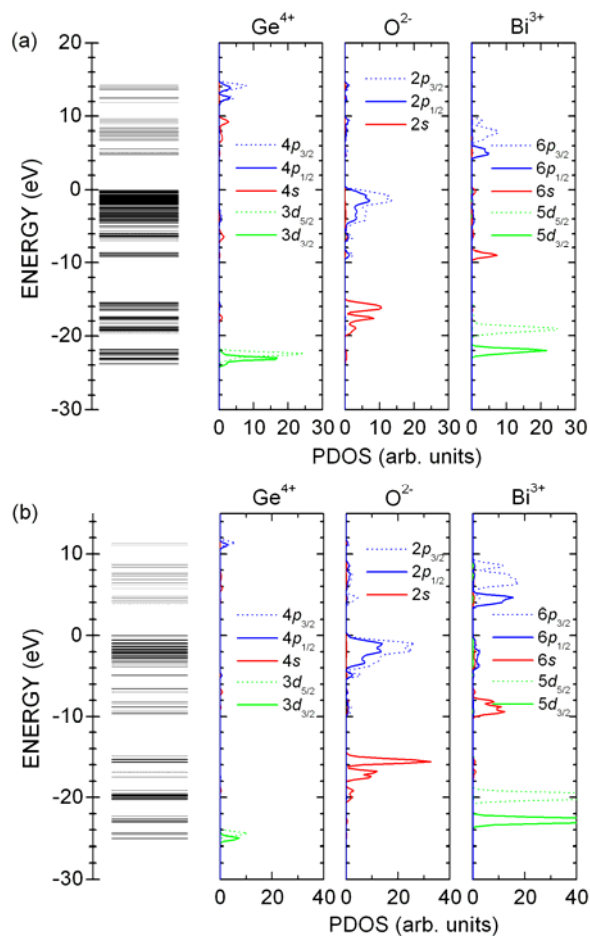


**Figure 5** Energy diagrams and PDOS curves of (a) e-BGO and (b) s-BGO calculated by the DV- $X\alpha$  method.

**5 Discussion** The lowest-energy band peaking at 4.81 eV in the reflection spectrum of e-BGO has been assigned to the Bi 6s  $\rightarrow$  6p transition.[3] This assignment is consistent with the previous theoretical proposal,[7] but not with the very recent calculation.[8] The present DV- $X\alpha$  calculation of e-BGO indicates that the top of the valence band is formed by the O 2p state with significant contribution from the Bi 6s state and the bottom of the conduction band is mainly formed by the Bi 6p state, and therefore supports the interpretation that the lowest reflection band

at 4.81 eV is due to the  $6s \rightarrow 6p$  transition of  $\text{Bi}^{3+}$  ions.

The 4.81 eV band is followed by a weak band peaking at 5.15 eV, which was not clearly observed in Ref. [3]. When  $T$  is increased from 5 to 300 K, the 4.81 and 5.15 eV bands are considerably broadened, the latter merging into the low-energy part of a broad band at around 6.25 eV. This feature reveals that these two bands are related to the excitonic transitions; i.e., the 4.81 and 5.15 eV bands are ascribed to the  $n = 1$  and  $n = 2$  excitons, respectively. Two-photon excitation spectrum of the e-BGO luminescence has been found to rise steeply at around 5.1 eV at LNT,[5] which is fairly compatible with the present assignment of the  $n = 2$  exciton peak.

Assuming the simple hydrogen-like model of exciton, the energy of the  $n$ th level,  $E_n$ , is expressed as  $E_n = E_g - E_B/n^2$ , where  $E_B$  is the exciton binding energy. By substituting the values of  $E_1$  and  $E_2$ , we obtain  $E_g = 5.26$  eV at 5 K and 5.17 eV at 300 K for e-BGO. The value of  $E_B$  is thus estimated to be  $0.45 \pm 0.02$  eV at 5 and 300 K.

Based on the similarity to e-BGO, we assign the lowest reflection band at 3.65 eV in s-BGO to the excitonic  $6s \rightarrow 6p$  transition of  $\text{Bi}^{3+}$  ions. This band is indeed broadened with increasing  $T$ . The present DV- $X\alpha$  calculation of s-BGO indicates that the uppermost valence band is substantially built up by the O 2p state with small contribution from the Bi 6s state. This could explain the fact that the oscillator strength of the 3.65 eV exciton band in s-BGO is smaller than that of the 4.81 eV band in e-BGO. The  $n = 2$  exciton peak is not observed in s-BGO. The value of  $E_g$  is roughly determined to be 3.8 eV from the beginning of the rise of the reflectivity after the excitonic band. We thus obtain  $E_B \approx 0.15$  eV for s-BGO.

The exciton binding energy is given as  $E_B = \mu e^4/2\hbar^2 \epsilon_\infty^2$ , where  $\mu$  is the reduced exciton mass,  $e$  the electron charge,  $\hbar$  the Planck constant, and  $\epsilon_\infty$  the optical dielectric constant. Since  $\epsilon_\infty = 4.67$  for e-BGO and 7.13 for s-BGO,[14] one may expect  $E_B(\text{s-BGO})/E_B(\text{e-BGO}) \approx 0.4$  if the value of  $\mu$  is assumed to be the same in both BGOs. The present result is in satisfactory agreement with this expectation.

Interpretations of the reflection structures above the band gap in e-BGO and s-BGO have been given in Refs. [3] and [10], respectively. These earlier interpretations are supported by our theoretical results of Figs. 5(a) and 5(b).

The 510 nm luminescence in e-BGO has been assigned to the  $6p (^3P_1) \rightarrow 6s (^1S_0)$  transition of  $\text{Bi}^{3+}$ . [4] No detailed measurement of the s-BGO luminescence has been done to date. In the present study, we found an emission band at 450 nm in s-BGO at 5 K. The excitation threshold of this luminescence is around 3.44 eV (360 nm), which coincides with the low-energy tail region of the exciton band. Such coincidence suggests that the 450 nm luminescence is intrinsic to s-BGO and originates from the radiative  $6p (^3P_1)$

$\rightarrow 6s (^1S_0)$  transition of  $\text{Bi}^{3+}$ , as in the case of e-BGO. To our knowledge, this is the first observation of the intrinsic luminescence in s-BGO.

As  $T$  is increased from 5 K, the intensity of the 450 nm emission band begins to decrease at 20 K, and vanishes above 50 K. This thermal quenching is fitted by using the Mott formula:  $I(T) = I(0)/[1 + C \cdot \exp(-\Delta E/k_B T)]$ , where  $C$  is the constant and  $\Delta E$  the activation energy. From the fit, we obtain  $\Delta E = 12$  meV and  $C = 165$ .

The luminescence yield of s-BGO is much weaker than that of e-BGO. This is explained in terms of relatively small contribution of the Bi 6s state to the top of the valence band in the former, as well as the oscillator strength of the exciton band. Here, it is implied that the luminescence process takes place in  $\text{Bi}^{3+}$  ions; radiative decay of a self-trapped exciton localized at  $\text{Bi}^{3+}$ . The self-trapped exciton spontaneously deforms the surrounding lattice. The difference in degree of the lattice deformation leads to the difference in the Stokes shift between e-BGO and s-BGO.

There may, however, be the possibility that a hole left behind in the valence band moves quickly from Bi to O site, especially in s-BGO, because the O 2p state mainly contributes to the uppermost valence band. If this is the case, the intrinsic BGO luminescence arises from the radiative recombination of an electron at  $\text{Bi}^{3+}$  and a hole at  $\text{O}^{2-}$ . It will be interesting to investigate whether the hole localizes at  $\text{Bi}^{3+}$  or  $\text{O}^{2-}$ .

**Acknowledgements** The authors would like to thank Y. Takizawa for his assistance in the experiments of e-BGO. A part of the present study was supported by the Joint Studies Program of the Institute for Molecular Science, Okazaki.

## References

- [1] M.J. Weber, *J. Lumin.* **100**, 35 (2002).
- [2] P.V. Lenzo, E.G. Spencer, and A.A. Ballman, *Phys. Rev. Lett.* **19**, 641 (1967).
- [3] F. Antonangeli, N. Zema, and M. Piacentini, *Phys. Rev. B* **37**, 9036 (1988).
- [4] M.J. Weber and R.R. Monchamp, *J. Appl. Phys.* **44**, 5495 (1973).
- [5] M. Casalboni, R. Francini, U.M. Grassano, C. Musilli, and R. Pizzoferrato, *J. Lumin.* **31/32**, 93 (1984).
- [6] F. Rogemond, C. Pedrini, B. Moine, and G. Boulon, *J. Lumin.* **33**, 455 (1985).
- [7] R. Moncorge, B. Jacquier, G. Boulon, F. Gaume-Mahn, and J. Janin, *J. Lumin.* **12/13**, 467 (1976).
- [8] M.V. Lalic and S.O. Souza, *Opt. Mater.* **30**, 1189 (2008).
- [9] R.B. Lauer, *Appl. Phys. Lett.* **17**, 178 (1970).
- [10] Sh. M. Éfendiev, A.M. Mamedov, V.É. Bagiev, and G.M. Éivazova, *Sov. Phys. Tech. Phys.* **26**, 1017 (1981).
- [11] J. Gironnet, V.B. Mikhailik, H. Kraus, P. de Marcillac, N. Coron, *Nucl. Instrum. Methods Phys. Res. A* **594**, 358 (2008).
- [12] I.V. Kityk, M.K. Zamorskii, and J. Kasprczyk, *Physica B* **226**, 381 (1996).

- [13] H. Adachi, M. Tsukada, and C. Satoko, *J. Phys. Soc. Jpn.* **45**, 875 (1978).
- [14] O.M. Bordun, I.I. Kukharskii, T.M. Yaremchuk, and S.I. Gaidai, *J. Appl. Spectrosc.* **71**, 382 (2004).